Population Balance Modeling and Simulation of Liquid–Liquid–Liquid Phase Transfer Catalyzed Synthesis of Mandelic Acid From Benzaldehyde

P. R. Sowbna and Ganapati D. Yadav
Dept. of Chemical Engineering, Institute of Chemical Technology (ICT), Nathalal Parekh Marg, Matunga, Mumbai 400019, India

Doraiswami Ramkrishna
School of Chemical Engineering, Purdue University, West Lafayette, IN

DOI 10.1002/aic.13780
Published online March 14, 2012 in Wiley Online Library (wileyonlinelibrary.com).

Mandelic acid has cosmetic, pharmaceutical, and antibacterial activities and is used in urinary antiseptic medicines. An attractive process for the production of mandelic acid is through reaction between benzaldehyde, sodium hydroxide, and chloroform in the presence of polyethylene glycol 4000 as a phase transfer catalyst. The liquid–liquid phase transfer catalyzed (L–L PTC) reaction can be intensified by converting it into three-liquid phases (L–L–L PTC). We address the modeling of a well-stirred reactor for the foregoing process, in which organic droplets surrounded by a thin film of catalyst-rich phase are suspended in the aqueous phase. A population balance model is formulated for the L–L–L PTC reaction and solved by Monte Carlo simulation using interval of quiescence technique. Transport processes and intrinsic reaction kinetics are extracted from the experiments. This population balance model serves to assess and interpret the relative roles of various processes in L–L–L PTC reaction, such as diffusive transport, reaction, and interaction between dispersed phase droplets. The model is expected to be an effective tool for reactor design and scale up. © 2012 American Institute of Chemical Engineers *AIChE J,* 58: 3799–3809, 2012

Keywords: phase transfer catalysis (PTC), liquid–liquid–liquid phase transfer catalysis (L-L PTC), population balance, mandelic acid, Monte Carlo simulation, interval of quiescence technique

Introduction

Phase transfer catalysis (PTC) has been used in more than 800 processes, particularly as liquid–liquid (L–L) and solid–liquid (S–L) systems for the past 40 years. However, only recently the importance of liquid–liquid–liquid (L–L–L) PTC has been demonstrated as a powerful method vis-à-vis biphasic PTC in commercially relevant reactions.[1–17] The translation of L–L PTC into L–L–L PTC renders several benefits. In L–L–L PTC, the middle phase is the catalyst-rich phase which is the main locale of the reaction into which both aqueous and organic phase reagents are transferred from the two interfaces. A typical L–L–L PTC consists of an organic phase dispersed as spherical drops, surrounded by a thin film of catalyst phase, within an aqueous continuous phase. There could be another situation where the inner phase is aqueous and the outer phase organic depending on density difference. The reaction rate depends on the concentration of the reacting species in the organic droplet and in the catalyst film at the middle at any instant of consideration. L–L–L PTC facilitates easier recovery and reuse of the catalyst-rich phase, enhancement in reaction rate, improvement in selectivity, and also reuse of the aqueous phase, leading to considerable reduction of waste and overall process intensification.

In L–L–L PTC system, during agitation, unstable dispersed droplets are formed and a dynamic process of coalescence and redispersion goes on continuously; these two processes influence the overall conversion and reaction rate by altering the interfacial area and rate of rejuvenation available for species exchange between the phases. Thus, it appears that tri-liquid PTC should be amenable to population balance modeling and simulation. The framework of population balances has been widely used to study the process of drop coalescence and redispersion.[18–22] In the population balance, the events of each individual drop are taken into account. Population balances lead to integro-differential equations that are frequently difficult to solve. Alternatively, information about the particulate system can be obtained by Monte Carlo simulation method,[18] which involves use of appropriate random number generating techniques.

The simulation procedure discussed by Shah et al.[22] is free from procedures of arbitrary discretization of the time interval and efficiently handles the stochastic behavior of small systems; it uses the concept of interval of quiescence technique (IQ) in Monte Carlo simulation of population balances.

D. Ramkrishna is the M.M. Sharma Distinguished Professor at ICT, Mumbai.

Correspondence concerning this article should be addressed to G. D. Yadav at gdyadav@yahoo.com, gd.yadav@ictmumbai.edu.in.

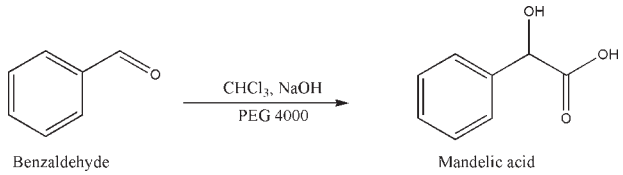

Scheme 1. Synthesis of mandelic acid from benzaldehyde.

The motivation for this article is modeling of the process for synthesis of mandelic acid using L–L–L PTC. Mandelic acid is an important ingredient in urinary antiseptic medicines. Further, its cosmeceutical and antibacterial properties make it a product of considerable commercial significance.

An attractive process for the production of mandelic acid is through the reaction between benzaldehyde and sodium hydroxide and chloroform (dichlorocarbene reaction) in the presence of polyethylene glycol (PEG) 4000 as catalyst using L–L–L PTC (Scheme 1). This process involves distribution of dispersed phase droplets with chemical reaction in a thin catalyst layer on each drop. Conversion and selectivity depend on dispersed phase mixing, transport of reaction species across the two interfaces to and within the droplet, and chemical reaction. Consequently, population balance methodology is an appropriate modeling tool for L–L–L PTC. Such an investigation has been done by Hibbard and Ramkrishna[22] for the simpler situation in L–L PTC system. In view of the importance of phase transfer catalysis for various other organic products, the analysis in this article would serve as an example for such applications.

The application of population balances to L–L–L PTC involves several complications. First, the dispersion process of droplet coalescence and redispersion leads to integro-differential equations involving coalescence and breakage kernels that are often unknown. Second, the reaction system involves several species requiring multidimensional population densities in several internal coordinates. Third, transport of reaction species to and within the droplets adds to the foregoing complications. Hence, the current model development is based on a hierarchy of simplifications described below.

Following an early (and interesting) idea of Curl,[23,24] we view the two processes of coalescence and breakage of droplets as a single step. Although this is an oversimplification, it does provide an efficient route to assessing the effects of drop mixing and redispersion. Curl assumed all drops to be of the same size equal to the average in the dispersion. Bajpai et al.[25] incorporated size dependence proposing that a pair of drops of different sizes coalesce and immediately redisperse into droplets of perfectly random size. The drop-size distribution is preserved by such interactions to be an exponential-size distribution which is found to be consistent with numerous studies. We confirm this observation with fresh experiments for the new system in our case.[26] The coalescence (or more appropriately ''interaction'') frequency is assumed to be independent of drop size but dependent on the stirrer speeds. This transient evolution of drop size is postulated to occur when the total number density of droplets is constant.[26]

Experiments were conducted following a protocol designed to extract model parameters from collected data, which will be useful for reactor design and scale up. Monte Carlo simulation using MATLAB was carried out to solve the population balance equation.

Experimental

Diffusion coefficients of benzaldehyde in the organic phase and the catalyst (middle) phase were determined experimentally as given below. The rate constant for the conversion of benzaldehyde to mandelic acid was also determined independently in an experiment free of transport effects and it was used in solving the population balance model. The rate constant for the conversion of benzaldehyde to benzoic acid was determined from experiments described in sections below and was used for estimating the diffusion coefficient of benzaldehyde in organic phase from the experiment for this section described below, as diffusion and reaction occurred together.

Materials

Benzaldehyde, chloroform, hexane, undecane, diethyl ether, sodium hydroxide, sodium sulfate of AR grade, acetonitrile, and acetic acid of HPLC grade and PEG 4000 were obtained from M/s. s.d.fine Chem., Mumbai, India.

Experimental setup and procedure

The synthesis of mandelic acid using L–L–L PTC was studied in a 4-cm inner diameter fully baffled mechanically agitated glass reactor of 100 cm^3 total capacity which was equipped with a standard six-blade-pitched turbine impeller. The reactor was kept in an isothermal water bath whose temperature could be maintained at a desired value.

Intrinsic kinetics for the conversion of benzaldehyde to benzoic acid in the presence of air

Typical runs were conducted in the same glass reactor with 0.01 mol benzaldehyde, 0.02 mol chloroform, 0.0025 mol undecane as internal standard dissolved in hexane to make the volume of organic phase to 20 cm^3. Organic phase in the presence of air was stirred and residual concentration of benzaldehyde in the organic phase was determined as a function of time.

Diffusion coefficient of benzaldehyde in organic phase

Benzaldehyde in stagnant organic layer was exposed to air. Benzaldehyde would diffuse to the surface and react with air forming benzoic acid. Typical runs were conducted with 0.01 mol benzaldehyde, 0.02 mol chloroform, and 0.0025 mol undecane as internal standard dissolved in hexane to make the volume of organic phase to 20 cm^3. The reaction mixture of the organic layer was taken in equal amount in five glass beakers of similar dimensions each containing the same composition. A zero sample was collected from all these beakers. The beakers were kept inside a constant temperature bath at 55°C. Samples were collected from each of the beakers at a time interval of 30 min. The first sample was collected from beaker 1 after 120 min of zero sampling. Then, the second sample was collected from beaker 2 after 180 min. In the same manner, samples were collected from beakers 3, 4, and 5 at an interval of 30 min. Analysis of the samples was done and the residual concentration of benzaldehyde in the organic phase was determined as a function of time.

Diffusion coefficient of benzaldehyde in catalyst phase

Typical runs were conducted in the same glass reactor with 0.01 mol benzaldehyde, 0.02 mol chloroform, 0.0025

mol undecane as internal standard dissolved in hexane to make the volume of organic phase to 20 cm^3. To this organic phase, 0.13 mol sodium chloride and 0.0007 mol PEG 4000 as a catalyst dissolved in water were added and the aqueous phase was made up to 20 cm^3 at 55°C. Three liquid phases were distinctly formed. The amount of PEG 4000 and sodium chloride determine the formation of third liquid phase. Diffusion of benzaldehyde from organic to the catalyst rich-phase occurs and no reaction occurs to produce mandelic acid. This set up was kept under nitrogen atmosphere to prevent the oxidation of benzaldehyde to benzoic acid. Gentle stirring of organic phase was done from the top without disturbing the bottom layers. Residual concentration of benzaldehyde in the organic phase was determined as a function of time.

Conversion of benzaldehyde to mandelic acid

The experimental setup and procedures were similar to those used to find the diffusion coefficient of benzaldehyde in the catalyst-rich phase, with a difference that the sodium chloride in the aqueous phase was replaced by 0.16 mol sodium hydroxide so that the conversion to mandelic acid would occur. Here, the amount of PEG 4000 and sodium hydroxide determine the formation of third liquid phase. Gentle stirring of organic phase was done from the top without disturbing the bottom layers. Residual concentration of benzaldehyde in the organic phase as a function of time was determined.

These experiments were repeated in the same experimental setup under nitrogen atmosphere. All three phases were well stirred at a given speed. The organic phase was seen as spherical droplets, surrounded by a thin film of catalyst phase, within an aqueous phase as the bulk continuous phase. The reactant benzaldehyde was added after the system reached the equilibrium distribution. The details are available elsewhere.[26]

The product mandelic acid was extracted *in situ* in the aqueous phase as sodium salt of mandelic acid. The aqueous phase was separated and neutralized with dilute HCl. The entire mixture was evaporated under vacuum to reduce the aqueous phase volume to 25 cm^3. This aqueous phase was saturated with sodium chloride. Then, the mandelic acid present in this aqueous phase was extracted with diethyl ether, which was dried with sodium sulfate and the solvent was evaporated to get solid mandelic acid and small amount of byproduct benzoic acid.

Method of analysis

Samples of the organic phase were analyzed by gas chromatography on a Chemito 8610 model. 10% SE 30 (4 m × 3.8 mm stainless steel packed column) was used in conjunction with flame ionization detector (FID). The conversion was based on disappearance of benzaldehyde. HPLC (Knauer, model K-501:63614) was used with a C-18 column and UV detector (Knauer, model K-501:62964) to analyze the above solid phase consisting of mandelic acid. The mobile phase composition was acetonitrile/water/acetic acid 60:39:1 by volume at a flow rate of 0.5 cm^3/min. UV detection wavelength was set at 231 nm. The product mandelic acid and byproduct benzoic acid found were confirmed by Liquid Chromatography Mass Spectrometry (LCMS) (Thermo electron Corporation-Finnigan LCQ Advantage MAX). Synthetic mixtures were also prepared for calibration and used to calculate the concentrations, reaction rates, and selectivity of mandelic acid.

Mathematical Modeling

Intrinsic kinetics for the conversion of benzaldehyde to benzoic acid in the presence of air

Intrinsic kinetics of the conversion of benzaldehyde to benzoic acid in the presence of air was obtained from the experimental data using a model equation

$$\bar{u} = e^{-\hat{k}_B t} \tag{1}$$

where $\hat{k}_B$, the rate constant for the conversion of benzaldehyde to benzoic acid could be determined from the slope of a plot of $\ln \bar{u}$ vs. t.

Diffusion coefficient of benzaldehyde in organic phase

The diffusion coefficient of benzaldehyde in the organic phase could be extracted from experimental data using the mathematical development of the process as given in Appendix A. The dimensionless concentration $\ln \bar{u}\ (\tau)$ is given by

$$\ln \bar{u}(\tau) \approx \ln \frac{2\beta^2}{\lambda_1\left(\lambda_1 + \beta^2 + \beta\right)} - \lambda_1 \tau \tag{2}$$

where λ_1 is the smallest root of the following (characteristic) equation

$$\tan \sqrt{\lambda} = \beta/\sqrt{\lambda} \tag{3}$$

Plotting $\ln \bar{u}\ (\tau)$ vs. t, gives the slope $(= -\lambda_1 D_B/\delta^2)$; combining this with the characteristic Eq. (3) and using the $\hat{k}_B$, D_B, the diffusion coefficient of benzaldehyde in organic phase, could be determined.

Diffusion coefficient of benzaldehyde in catalyst-rich phase

Diffusion coefficient of benzaldehyde in the catalyst-rich phase was obtained from the experimental data via the model equation (for detailed derivation, refer Appendix B).

$$u_1(\tau) - \frac{1}{(1+\gamma)} \approx \cos\sqrt{\lambda_1}\left[\frac{1}{2}\left(1 + \frac{(1-\gamma)}{(\gamma + \lambda_1/\gamma)}\right)\right]^{-1} e^{-\lambda_1 \tau} \tag{4}$$

The eigenvalue λ_1 must satisfy the characteristic Eq. (B24) (Appendix B)

A plot of $\ln [u_1(\tau) - (1+\gamma)^{-1}]$ vs. t provides, for large enough τ, a straight-line of slope $(= -\lambda_1 D_{Bc}/\delta_c^2)$, from which the diffusion coefficient D_{Bc} can be determined.

Rate constant for conversion of benzaldehyde to mandelic acid

The characteristic equation is given by (detailed derivation is available in Appendix C)

$$\tan\ \sqrt{\lambda + \kappa} = -\frac{\lambda}{\gamma\sqrt{\lambda + \kappa}} \tag{5}$$

Rate constant for the conversion of benzaldehyde to mandelic acid could be obtained from the model equation (for derivation, refer Appendix C)

$$u_1(\tau) \approx \frac{(\lambda_1 + \kappa)e^{-\lambda_1 \tau}}{3\gamma^2(\lambda_1 + \kappa) + \lambda_1(\lambda_1 - \gamma)} \tag{6}$$

Thus, plotting $\ln u_1(\tau)$ vs. τ (for large enough τ) gives a slope of $-\lambda_1$. Substituting the value λ_1 in the characteristic Eq. (5)

will yield the value of κ. As all other parameters are known, k_B, the reaction rate constant can be determined.

Model for dispersed phase mixing and reaction

For dispersed phase mixing and reaction, when diffusion effects were accountable, the characteristic equation for the eigenvalues is derived as follows (detailed derivation available in Appendix D)

$$\sqrt{\lambda}\cot\sqrt{\lambda} - 1 = \frac{\theta}{K}\frac{\left[\varepsilon\sqrt{\frac{\lambda}{\theta}-\kappa}\cot\left(\varepsilon\sqrt{\frac{\lambda}{\theta}-\kappa}\right) - \left\{1+(1+\varepsilon)\sqrt{\frac{\lambda}{\theta}-\kappa}\right\}\right]}{\left[1-(1+\varepsilon)\sqrt{\frac{\lambda}{\theta}-\kappa}\cot\left(\varepsilon\sqrt{\frac{\lambda}{\theta}-\kappa}\right)\right]} \quad (7)$$

When the diffusion effects become negligible, the concentration in each droplet at any instant of time can be calculated from the following equation (detailed derivation available in Appendix D).

$$\bar{u}(\tau) = \exp\left[-\tau\frac{\kappa\{3\varepsilon(1+\varepsilon+\varepsilon^2/3)\}}{K+\{3\varepsilon(1+\varepsilon+\varepsilon^2/3)\}}\right] \quad (8)$$

Population Balance and Monte Carlo Method of Simulation

Population balance equation

Transient drop sizes are associated with transient reactant concentration distribution among the drop population on which the overall conversion would depend. The prediction of such effects can be made with the population balance analysis. In the population balance analysis, each drop is considered as a reactor and the overall reaction rate at any instant is the cumulative result of reaction rates in individual droplets. In a very short computation time, L–L–L PTC reaction system can be visualized.

Based on the models of Bajpai et al.[25] and Hibbard and Ramkrishna,[22] the basic assumptions considered in the formulation of the population balance here are:

1. Particle events, that is, coalescence and redispersion are not influenced by solute concentration, mass transfer or chemical reaction,
2. Only one particulate event occurs, that is, two droplets coalesce, mix completely then immediately redisperse into two daughters according to a uniform distribution, the only requirement being volume conservation,
3. If the model for particle events conforms to "the coalescence followed by immediate redispersion," the total number of droplets must remain constant throughout.

The population balance equation for the foregoing situation has been described elsewhere.[26,27]

Following the published procedure,[21] the concept of IQ in the Monte Carlo simulation was used for solving this population balance model using MATLAB.

Simulation of dispersed phase coalescence and redispersion

Initial distribution of droplets volumes were generated using exponential random number generator of MATLAB. The initial condition of a particulate system might be specified by fixing the properties of the individual droplets in the system. To implement the IQ technique, exponential random number generator of MATLAB was used to generate an IQ.

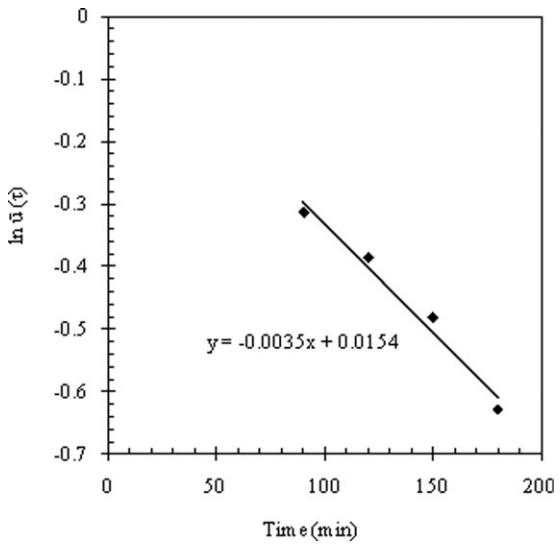

Figure 1. Measurement of intrinsic kinetics of conversion of benzaldehyde to benzoic acid.

Selection of two droplets which coalesce is completely random. Each droplet had equal probabilities to participate in each particulate event, as the coalescence frequency was constant for a particular speed of agitation. The uniform random number generator of MATLAB was used to select the two droplets that coalesce from the sample. The volumes of the new droplets formed due to redispersion were also uniformly distributed and the daughter droplets volumes were found out using uniform random number generator of MATLAB.

Simulation of dispersed phase chemical reaction

The concentration of reactants in each drop changes with time, and thus, the concentrations in all droplets were updated after each particulate event. The cycle of generating an IQ, updating the sample, and enacting a particulate event were continued till the end point. This complete cycle formed one sample path. Additional sample paths were generated in the same manner. With this concept of IQ technique, the particulate events were simulated using MATLAB and the concentrations of all the droplets were updated according to the proposed model for dispersed phase reaction, Eq. (8).

Results and Discussion

Intrinsic reaction kinetics and transport processes

Figure 1 shows the plot of ln $\overline{u}$ vs. t for the conversion of benzaldehyde to benzoic acid to establish the kinetics. The reaction rate constant, $\hat{k_B}$, was found from the slope as 0.0035 min^{-1}, which is used in the determination of diffusion coefficient of benzaldehyde in organic phase.

Figure 2 shows the plot of ln $\overline{u}$ vs. t for the experiment conducted to extract the diffusion coefficient of benzaldehyde in organic phase, which yields a slope of $\frac{-\lambda_1 D_B}{\delta^2}$, which on combination the characteristic Eq. (3) and $\hat{k_B}$, the diffusion coefficient of benzaldehyde in organic phase, D_B, was determined as 2.12×10^{-5} cm^2/s. This is in close agreement with the value 2.88×10^{-5} cm^2/s, which was predicted using the Wilke–Chang equation.

Diffusion coefficient of benzaldehyde in the catalyst-rich phase was obtained using the model as 1.76×10^{-7} cm^2/s (Figure 3). The value predicted by Wilke–Chang equation was 0.92×10^{-7} cm^2/s. Such deviation was expected

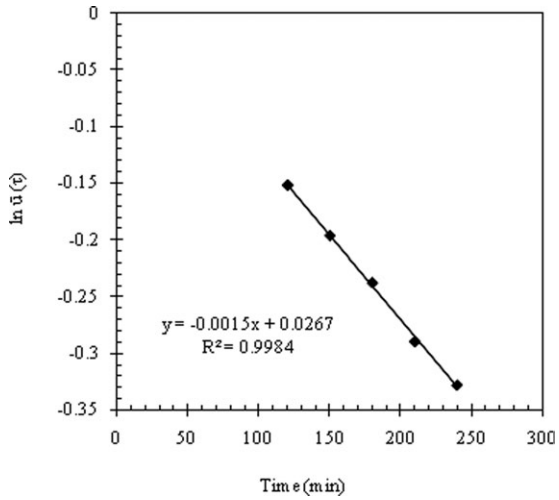

Figure 2. Measurement of diffusion coefficient of benzaldehyde in organic phase.

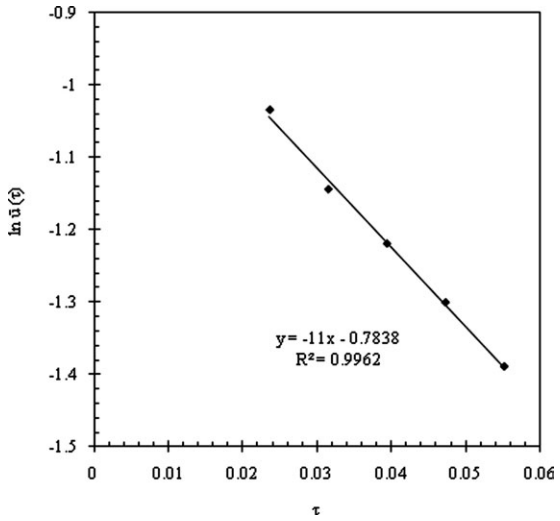

Figure 4. Measurement of intrinsic kinetics for the conversion of benzaldehyde to mandelic acid.

because some of the parameters used in this calculation were approximate values.

The intrinsic rate constant for the conversion of benzaldehyde to mandelic acid was obtained using the model as 0.1606 min^{-1} (Figure 4). This is in close agreement with the value 0.1537 min^{-1} obtained by the experiment conducted under the condition of dispersed phase mixing and reaction.[26] The selectivity toward mandelic acid was found to be 98%.

In the case of the model for dispersed phase mixing and reaction, Eqs. (D30) and (8) are the final solutions of the model when diffusion effects were accountable and when diffusion effects were negligible, respectively. For the first case, the smallest eigenvalue λ_1 was calculated for the mean drop size at 1000 rpm using Eq. (7). For the second case, the quantity $\frac{\kappa\{3\varepsilon(1+\varepsilon+\varepsilon^2/3)\}}{K+\{3\varepsilon(1+\varepsilon+\varepsilon^2/3)\}}$ in Eq. (8) was calculated. Both are in close agreement which showed that there was no mass-transfer resistance.

The Damkohler number, N_D, which is the ratio of characteristic diffusion time to characteristic reaction time, was found to be very low; it also showed that there was no mass-transfer resistance. Therefore, that model based on uniform concentration of benzaldehyde in both organic phase and catalyst phase as given by Eq. (8) was used to update the concentration of all the droplets after each particulate event in the simulation. All previous studies on a variety of reactions involving L–L–L PTC have reported an enhancement in the conversion when the third liquid phase (catalyst phase) appears.[1–17] This shows the catalyst-rich phase around the drop, where the reaction occurs, plays an important role in the conversion; hence, the film thickness cannot be neglected. The variation of film thickness with the radius of drop was determined and reported for this system.[26] These data were used while using the model for mixing and reaction for Monte Carlo simulation.

Population balance and Monte Carlo method of simulation

The effect of sample size and number of simulations was studied. The Monte Carlo method was used for 1500 simulations with a sample of 10 drops, and 500 simulations with sample of 50 drops. Figure 5 presents the comparison of

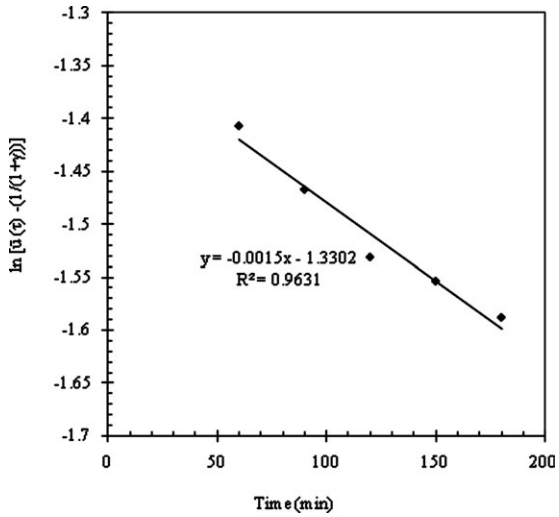

Figure 3. Measurement of diffusion coefficient of benzaldehyde in catalyst phase.

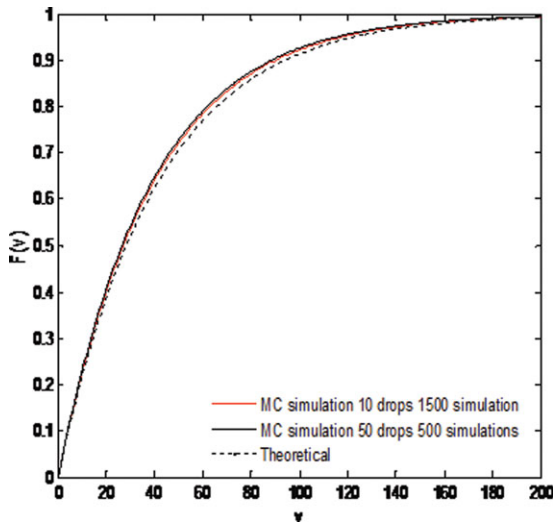

Figure 5. Cumulative distribution function by Monte Carlo simulation vs Theoretical cumulative distribution function at the end of reaction.

[Color figure can be viewed in the online issue, which is available at wileyonlinelibrary.com.]

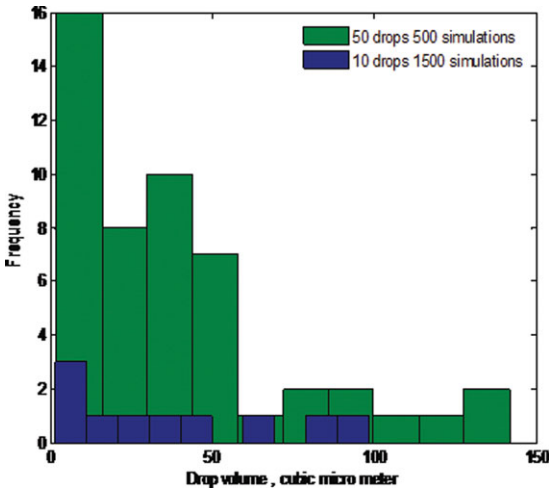

Figure 6. Histogram for simulated drop size distribution.

[Color figure can be viewed in the online issue, which is available at wileyonlinelibrary.com.]

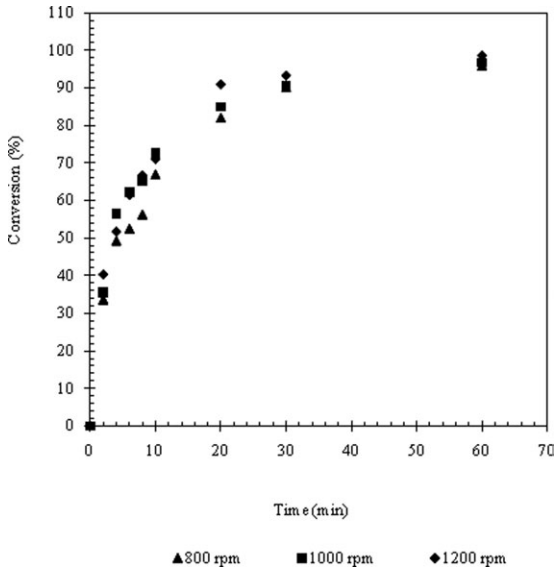

Figure 8. Effect of speed of agitation on conversion.

cumulative distribution function predicted by Monte Carlo simulation with the population balance at the end of reaction at 1000 rpm. The sample of 10 drops with 1500 simulations showed good quantitative agreement with the theoretical cumulative distribution function. Therefore, the rest of the results are shown for the sample of 10 drops with 1500 simulations.

Figure 6 shows the comparison of histograms obtained by Monte Carlo simulation for a sample of 50 drops with 500 simulations, and for a sample of 10 drops with 1500 simulations. This shows a good fit with the exponential distribution.

Cumulative distribution function was also calculated for different speeds of agitation (Figure 7). The model predicts that increase in agitation speed leads to smaller drop sizes and less variation in the distribution. It was observed from the population balance analysis that droplet-size distribution varies significantly between 800 and 1000 rpm, whereas it is close to each other for 1000 and 1200 rpm (Figure 7). Mass-transfer resistance was present at speed of agitation of 800, which marginally decreased at 1000 rpm; beyond which it was eliminated. This is in agreement with the experimental results. The conversion and selectivity were practically the same at 1000 and 1200 rpm (Figure 8, Table 1). The optimum speed of agitation was 1000 rpm which is directly proportional to the optimum power consumption. The extent to which the mixing affects, the conversion and selectivity could be analyzed by the population balance model.

The model was used to predict the effects of drop-size distribution, droplets coalescence and redispersion on

Table 1. Effect of Speed of Agitation on Selectivity

Speed of Agitation (rpm)	Selectivity to Mandelic Acid (%)
800	97
1000	98
1200	98

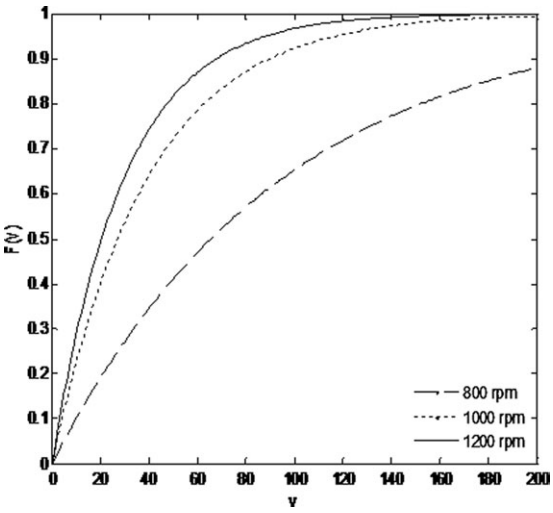

Figure 7. Cumulative distribution function as a function of speed of agitation.

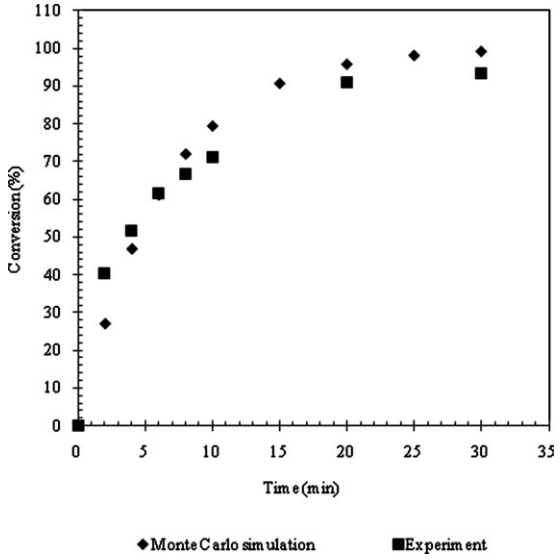

Figure 9. Conversion with time at 1000 rpm.

conversion for reacting dispersions. The apparent approach of reaction conversion to the steady-state value is evident from Figure 9, which compares the results predicted by Monte Carlo simulation, the experimental data at 1000 rpm. The predictions by Monte Carlo simulation at 1000 and 1200 rpm are also in reasonable agreement with the experimental data.

Conclusions

The novelty of the L–L–L PTC reactions is that the catalyst rich phase can be repeatedly reused, and it intensifies the rates of reaction and improves the selectivity of the desired product. In turn, it leads to the reduction of waste. This catalyst-rich phase is the main reaction phase. However, conversion and selectivity depend on dispersed phase mixing, transport of reaction species to and within the droplets, and chemical reaction. A mathematical model based on population balance equation was proposed to describe the dynamics of droplet dispersion and reaction in L–L–L PTC system; and Monte Carlo simulation was performed using the concept of IQ. Synthesis of mandelic acid from the reaction of benzaldehyde with dichlorocarbene using PEG 4000 as phase transfer catalyst was considered as a model reaction.

The model parameters like rate constant and diffusion coefficient of benzaldehyde in organic phase and in catalyst-rich phase were extracted from the experimental data. These model parameters were used in the population balance analysis. A comparison of simulated values of conversion with experimental data indicates that there is an excellent agreement between them. Thus, the population balance model is an effective tool to evaluate the transient effects of transport, mass transfer, and reaction rate processes, and droplet dispersion processes on product conversion and selectivity in L–L–L PTC.

The L–L–L PTC reaction for the conversion of benzaldehyde to mandelic acid was studied using population balance analysis when there was no mass transfer limitation. If mass-transfer resistance is significant, the computation can be modified to account for it, while updating the concentration in the droplets. A significant advantage is that in a very short computation time, the L–L–L PTC reaction system can be visualized. This population balance analysis can be applied to other L–L–L PTC systems with the modification only in the model parameters.

The experimental measurement of micromixing is very difficult in contrast to that of macromixing. If the measurements inside the vessel are needed on pilot or commercial scale, it is practically impossible. However, in such cases population balance analysis could be used. In population balance analysis for L–L–L PTC system, droplets are pictured at any instant of time, which provides information on the coalescence event and can identify the coalescing pair of droplets, sizes of individual droplets, their concentration, the catalyst film thickness and its effect on conversion. These predictions due to the population balance analysis provide a great insight in the L–L–L PTC reactions which are useful for reactor design and scaleup.

Acknowledgments

PRS thanks University Grant Commission, India for an award of SRF. GDY acknowledges support from R. T. Mody Distinguished Professor Endowment and J. C. Bose National Fellow from DST-GOI and DR received support as M. M. Sharma Distinguished Professor of Chemical Engineering at ICT.

Notation

A = interfacial area between organic and catalyst phase
c_B = concentration of benzaldehyde in organic phase
C_{B_0} = initial Concentration of benzaldehyde in organic phase
c_B = concentration of benzaldehyde in catalyst phase
D_B = diffusion coefficient of benzaldehyde in organic phase
D_{Bc} = diffusion coefficient of benzaldehyde in catalyst phase
k_B = rate constant for the conversion of benzaldehyde to benzoic acid
k_B = rate constant for the conversion of benzaldehyde to mandelic acid
K = equilibrium distribution coefficient
n = population density
R = radius of drop
V = volume of organic phase
v = drop volume
v_c = catalyst volume
δ = thickness of organic phase
δ_c = thickness of catalyst phase
ω = coalescence frequency
λ = root of the equation
τ, u, x, β, γ, κ, ε, θ = dimensionless variables

Literature Cited

1. Yadav GD, Naik SS. Novelties of liquid–liquid–liquid phase transfer catalysis alkoxylation of p-chloronitrobenzene. *Catal Today*. 2001;66:345–354.
2. Yadav GD, Naik SS. Solid-liquid phase transfer catalyzed methoxylation of chloronitrobenzenes to nitroanisoles, *Org Proc Res Dev*. 1999;3:83–91.
3. Yadav GD, Bisht PM. Selectivity engineering in multiphase transfer catalysis in the preparation of aromatic ethers. *J Mol Catal A: Chem*. 2004;223:93–100.
4. Yadav GD, Lande SV. Liquid-liquid-liquid phase transfer catalysis: a novel and green concept for selective reduction of substituted nitroaromatics. *Adv Synth Catal*. 2005;347:1235–1241.
5. Yadav GD, Lande SV. Novelties of reaction in the middle liquid phase in tri-liquid phase transfer catalysis: kinetics of selective O-alkylation of vanillin with benzyl chloride. *Appl Catal. A: Gen*. 2005;287:267–272.
6. Yadav GD, Badure OV. Role of third phase in intensification of reaction rates and selectivity: phase-transfer catalyzed synthesis of benzyl phenyl ether. *Ind Eng Chem Res*. 2007;46:8448–8458.
7. Yadav GD. Insight into green phase transfer catalysis. *Top Catal*. 2004;29:145–161.
8. Yadav GD, Lande SV. Intensification of rates and selectivity using tri-liquid versus bi-liquid phase transfer catalysis: Insight into reduction of 4-nitro-o-xylene with sodium sulfide. *Ind Eng Chem Res*. 2007;46:2951–2961.
9. Yadav GD, Reddy CA. Kinetics of the n-butoxylation of p-chloronitrobenzene under liquid-liquid-liquid phase transfer catalysis. *Ind Eng Chem Res*. 1999;38:2245–2253.
10. Yadav GD, Jadhav YB, Sengupta S. Selectivity engineered phase transfer catalysis in the synthesis of fine chemicals: reactions of p-chloronitrobenzene with sodium sulphide. *J Mol Catal A: Chem*. 2003;200:117–129.
11. Yadav GD, Badure OV. Selective engineering in O-alkylation of m-cresol with benzyl chloride using liquid–liquid–liquid phase transfer catalysis. *J Mol Catal A: Chem*. 2008;288:33–41.
12. Yadav GD, Desai NM. Selectivity engineering of phase transfer catalyzed alkylation of 2-hydroxy aectophenone: enhancement in rates and selectivity by creation of a third liquid phase. *Org Process Res Dev*. 2005;9:749–756.
13. Yadav GD, Motirale BG. Selective oxidation of methyl mandelate to methyl phenyl glyoxylate using liquid–liquid–liquid phase transfer catalysis. *Chem Eng J*. 2010;156:328–336.
14. Yadav GD, Desai NM. Novelties of low energy microwave irradiation in tri-phase vis-a-vis bi-liquid phase-transfer catalysis in selective etherification of aromatic phenols. *Catal Commun*. 2006;7:325–330.
15. Yadav GD, Badure OV. Selective engineering in O-alkylation of m-cresol with benzyl chloride using liquid–liquid–liquid phase transfer catalysis. *J Mol Catal A: Chem*. 2008;288:33–41.

16. Yadav GD, Sowbna PR. Selectivity engineering in synthesis of 4-benzyloxy propiophenone using liquid - liquid-liquid phase transfer catalysis, *Ind Eng Chem Res*. 2012;51:3256–3264.
17. Yadav GD, Sowbna PR. Modeling of microwave irradiated liquid–liquid–liquid (MILLL) phase transfer catalyzed green synthesis of benzyl thiocyanate, *Chem Eng J*. 2012;179:221–230.
18. Ramkrishna D. Analysis of population balance. IV: The precise connection between Monte Carlo simulation and population balances. *Chem Eng Sci*. 1981;36:1203–1209.
19. Ramkrishna D. *Population Balances-Theory and Applications to Particulate Systems in Engineering*, Academic Press: London, 2000.
20. Ramkrishna D, Mahoney AW. Population balance modelling: promise for the future, *Chem Eng Sci*. 2002;57:595–606.
21. Shah BH, Ramkrishna D, Borwanker JD. Simulation of particulate systems using the concepts of the interval of quiescence. *AIChE J*. 1977;23:897–904.
22. Hibbard JL, Ramkrishna D. Analysis of phase transfer catalytic reactions in liquid-liquid systems. Process and fundamental consideration of selected hydrometallurgical systems, New York, *Society of Mining Eng*. 1981; 281–289.
23. Curl, RL. Dispersed phase mixing. I: Theory and effects in simple reactors. *AIChE J*. 1963;9:175–181.
24. Curl RL. Dispersed phase mixing effects on second moments in dominantly first-order, back mix reactors. *Chem Eng Sci*. 1967;22:353–357.
25. Bajpai RK, Ramkrishna D, Prokop A. A coalescence redispersion model for drop size distribution in an agitated vessel. *Chem. Eng. Sci*. 1976;31:913–920.
26. Sowbna PR, Ph D (Tech) Thesis in Chemical Engineering, University of Mumbai, Mumbai, India, 2011.
27. Ramkrishna D. The status of population balances. *Rev Chem Eng*. 1985;3:49–95.
28. Ramkrishna D. Operator-theoretic methods in heat and mass transfer problems. In: Majumdar AS, Mashelkar RA (Ed). Advances in Transport Processes. Wiley Eastern, Delhi. 1983;3:387–435.

Appendix A

Diffusion coefficient of benzaldehyde in organic phase

The transport reaction problem is defined as follows

$$\frac{\partial c_B}{\partial t} = D_{\mathrm{B}} \frac{\partial^2 c_{\mathrm{B}}}{\partial y^2}, \quad 0<y<\delta, \quad t > 0 \tag{A1}$$

$$y = 0, \quad D_{\mathrm{B}} \frac{\partial c_{\mathrm{B}}}{\partial y} = \hat{k}_{\mathrm{B}} c_{\mathrm{B}}, \quad y = \delta, \quad \frac{\partial c_{\mathrm{B}}}{\partial y} = 0 \tag{A2}$$

$$t = 0, \quad c_{\mathrm{B}} = c_{\mathrm{B_o}}, \quad 0<y<\delta \tag{A3}$$

Using dimensionless variables as follows

$$x \equiv \frac{y}{\delta}, \quad \tau \equiv \frac{D_{\mathrm{B}} t}{\delta^2}, \quad u(x,\tau) \equiv \frac{c_{\mathrm{B}}}{c_{\mathrm{B_o}}}, \quad \beta \equiv \frac{\hat{k}_{\mathrm{B}} \delta}{D_{\mathrm{B}}} \tag{A4}$$

The dimensionless boundary initial value problem becomes

$$\frac{\partial u}{\partial \tau} = \frac{\partial^2 u}{\partial x^2}, \quad 0<x<1, \quad \tau > 0 \tag{A5}$$

$$x = 1, \quad \frac{\partial u}{\partial x} = 0; \; x = 0, \quad \frac{\partial u}{\partial x} = \beta u \tag{A6}$$

$$\tau = 1, \quad u = 1, \quad 0<x<1 \tag{A7}$$

The above problem is readily solved in terms of eigenfunction expansion as follows. The eigenvalue problem is given by

$$z'' = -\lambda z, \quad z'(1) = 0, \quad z'(0) = \beta z(0) \tag{A8}$$

From which, we obtain

$$z(x) = A \cos \sqrt{\lambda}(1-x) \tag{A9}$$

where A is given by

$$A^2 = 1/\int_0^1 \cos^2 \sqrt{\lambda}(1-x)dx = 2/\int_0^1 \left[1 + \cos 2\sqrt{\lambda}(1-x)\right]dx \tag{A10}$$

The eigenvalues must satisfy the characteristic equation

$$\tan \sqrt{\lambda} = \beta/\sqrt{\lambda} \tag{A11}$$

Thus,

$$z(x) = \sqrt{\frac{2\left(\lambda+\beta^2\right)}{\left(\lambda+\beta^2+\beta\right)}} \cos \sqrt{\lambda}(1-x) \tag{A12}$$

The solution to the problem is given by

$$u(x,\tau) = \sum_{n=1}^{\infty} \frac{2\left(\lambda_n+\beta^2\right)e^{-\lambda_n \tau}}{\left(\lambda_n+\beta^2+\beta\right)} \cos \sqrt{\lambda_n}(1-x) \int_0^1 \cos \sqrt{\lambda_n}(1-x')dx' \tag{A13}$$

$$u(x,\tau) = \sum_{n=1}^{\infty} \frac{2\left(\lambda_n+\beta^2\right)e^{-\lambda_n \tau}}{\left(\lambda_n+\beta^2+\beta\right)} \frac{1}{\sqrt{\lambda_n}} \sin \sqrt{\lambda_n} \cos \sqrt{\lambda_n}(1-x) \tag{A14}$$

Measurements are made of the quantity

$$\bar{u}(\tau) \equiv \int_0^1 u(x,\tau)dx = \beta^2 \sum_{n=1}^{\infty} \frac{2e^{-\lambda_n \tau}}{\lambda_n\left(\lambda_n+\beta^2+\beta\right)} \tag{A15}$$

For large enough τ

$$\bar{u}(\tau) \approx \beta^2 \frac{2e^{-\lambda_1 \tau}}{\lambda_1\left(\lambda_1+\beta^2+\beta\right)} \tag{A16}$$

$$\ln \bar{u}(\tau) \approx \ln \frac{2\beta^2}{\lambda_1\left(\lambda_1+\beta^2+\beta\right)} - \lambda_1 \tau \tag{A17}$$

where λ_1 is the smallest root of the equation $\tan \sqrt{\lambda} = \beta/\sqrt{\lambda}$

Appendix B

Diffusion coefficient of benzaldehyde in catalyst-rich phase

The mathematical problem can be defined as follows

$$D_{\mathrm{Bc}} \frac{\partial^2 c'_{\mathrm{B}}}{\partial y^2} = \frac{\partial c'_{\mathrm{B}}}{\partial t}, \quad t > 0, \quad 0<y<\delta_c \tag{B1}$$

$$t = 0, \quad c'_{\mathrm{B}} = 0, \quad 0<y<\delta_c, \tag{B2}$$

$$y=\delta_c,\quad c'_{\mathrm{B}}=Kc_{\mathrm{B}};\quad V\frac{dc_{\mathrm{B}}}{dt}=-AD_{\mathrm{B}c}\frac{\partial c'_{\mathrm{B}}}{\partial y} \tag{B3}$$

$$y=0,\quad \frac{\partial c'_{\mathrm{B}}}{\partial y}=0\quad(\text{aqueous}-\text{catalyst interface}) \tag{B4}$$

$$t=0,\quad c_{\mathrm{B}}=c_{\mathrm{B}0}\quad(\text{in organic phase}) \tag{B5}$$

These are converted into dimensionless parameters as follows

$$x\equiv\frac{y}{\delta_c},\quad \tau\equiv\frac{D_{\mathrm{B}c}t}{\delta_c^2},\quad u(x,\tau)\equiv\frac{c'_{\mathrm{B}}}{Kc_{\mathrm{B}o}},\quad u_1\equiv\frac{c_{\mathrm{B}}}{c_{\mathrm{B}o}},\quad \gamma\equiv\frac{KA\delta_c}{V} \tag{B6}$$

$$\frac{\partial^2 u}{\partial x^2}=\frac{\partial u}{\partial\tau},\quad \tau>0,\quad 0<x<1 \tag{B7}$$

$$x=0,\quad \frac{\partial u}{\partial x}=0;\quad x=1,\quad -\gamma\frac{\partial u}{\partial x}=\frac{du_1}{d\tau},\quad u(1,\tau)=u_1(\tau) \tag{B8}$$

The problem can be cast following the methodology outlined in Ramkrishna[28] as follows; We define vector

$$\mathbf{f}\equiv\begin{bmatrix}f(x)\\ f_1\end{bmatrix},\ \mathbf{L}\equiv\{L,D(L)\};\ L\equiv\begin{bmatrix}-\frac{d^2}{dx^2} & 0\\ \gamma\left(\frac{d}{dx}\right)_{x=1} & 0\end{bmatrix}, \tag{B9}$$

$$D(L)=\{\mathbf{f}:f'(0)=0;f(1)=f_1\} \tag{B10}$$

Now, we can define

$$\mathbf{u}(\tau)\equiv\begin{bmatrix}u(x,\tau)\\ u_1(\tau)\end{bmatrix}\ \text{which makes}\ \mathbf{u}(\tau)\in D(L) \tag{B11}$$

The boundary value problem may be written as

$$\mathbf{L}\mathbf{u}(\tau)=-\frac{d\mathbf{u}}{d\tau},\quad \mathbf{u}(0)=\mathbf{u}_o\equiv\begin{bmatrix}0\\ 1\end{bmatrix} \tag{B12}$$

The inner product is defined by

$$\left\langle\mathbf{f},\mathbf{g}\right\rangle\equiv\int_0^1 f(x)g(x)dx+\frac{1}{\gamma}f_1g_1 \tag{B13}$$

which assures us that

$$\langle\mathbf{L}\mathbf{f},\mathbf{g}\rangle=\langle\mathbf{f},\mathbf{L}\mathbf{g}\rangle \tag{B14}$$

The eigenvalues of the operator $\mathbf{L}$ are obtained from

$$\mathbf{L}\mathbf{z}=\lambda\mathbf{z}\Rightarrow z''=-\lambda z,\quad \gamma z'(1)=\lambda z_1=\lambda z(1). \tag{B15}$$

$$z'(0)=0,\quad z(1)=z_1. \tag{B16}$$

$$z(x)=A\cos\sqrt{\lambda}x,\qquad z_1=A\cos\sqrt{\lambda} \tag{B17}$$

so that

$$\mathbf{z}_n\equiv A_n\begin{bmatrix}\cos\sqrt{\lambda_n}x\\ \cos\sqrt{\lambda_n}\end{bmatrix} \tag{B18}$$

$\lambda=0$ is also an eigenvalue with eigenvector

$$\mathbf{z}_o\equiv A_o\begin{bmatrix}1\\ 1\end{bmatrix}. \tag{B19}$$

The constant A_0 is obtained from

$$\left\langle\mathbf{z}_o,\mathbf{z}_o\right\rangle=1=A_o^2\left(1+\frac{1}{\gamma}\right) \tag{B20}$$

$$A_o=\left(1+\frac{1}{\gamma}\right)^{-1/2} \tag{B21}$$

The constants $\{A_n\}$ are obtained from

$$1=\left\langle\mathbf{z}_n,\mathbf{z}_n\right\rangle=A_n^2\left[\int_0^1\cos^2\sqrt{\lambda_n}xdx+\frac{1}{\gamma}\cos^2\sqrt{\lambda_n}\right]$$
$$=A_n^2\left[\frac{1}{2}\left(1+\frac{1}{2\sqrt{\lambda_n}}\sin 2\sqrt{\lambda_n}+\frac{1}{\gamma}\cos^2\sqrt{\lambda_n}\right)\right] \tag{B22}$$

$$A_n=\left[\frac{1}{2}\left(1+\frac{(1-\gamma)}{(\gamma+\lambda_n/\gamma)}\right)\right]^{-1/2} \tag{B23}$$

The eigenvalues must satisfy the characteristic equation

$$-\gamma\sqrt{\lambda}\sin\sqrt{\lambda}=\lambda\cos\sqrt{\lambda}\ \text{ or }\ \tan\sqrt{\lambda}=-\frac{\sqrt{\lambda}}{\gamma} \tag{B24}$$

which has infinite roots. The solution of the boundary initial value problem is given by

$$\mathbf{u}(\tau)=\left\langle\mathbf{u}_o,\mathbf{z}_o\right\rangle\mathbf{z}_o+\sum_{n=1}^{\infty}\left\langle\mathbf{u}_o,\mathbf{z}_n\right\rangle\mathbf{z}_n e^{-\lambda_n\tau} \tag{B25}$$

Measurements are being made of $u_1(\tau)$ which is given by

$$u_1(\tau)=\frac{1}{(1+\gamma)}+\sum_{n=1}^{\infty}\left[\frac{1}{2}\left(1+\frac{(1-\gamma)}{(\gamma+\lambda_n/\gamma)}\right)\right]^{-1}e^{-\lambda_n\tau}\cos\sqrt{\lambda_n} \tag{B26}$$

For large enough τ, we have the result

$$u_1(\tau)-\frac{1}{(1+\gamma)}\approx\cos\sqrt{\lambda_1}\left[\frac{1}{2}\left(1+\frac{\left(1-\gamma\right)}{(\gamma+\lambda_1/\gamma)}\right)\right]^{-1}e^{-\lambda_1\tau} \tag{B27}$$

Appendix C

Rate constant for conversion of benzaldehyde to mandelic acid

The mathematical formulation is

$$D_{\mathrm{B}c}\frac{\partial^2 c'_{\mathrm{B}}}{\partial y^2}-k_{\mathrm{B}}C'_{\mathrm{B}}=\frac{\partial c'_{\mathrm{B}}}{\partial t},\quad t>0,\quad 0<y<\delta_c \tag{C1}$$

$$t=0,\quad c'_{\mathrm{B}}=0,\quad 0<y<\delta_c, \tag{C2}$$

$$y=\delta_c,\quad c'_{\mathrm{B}}=Kc_{\mathrm{B}};\quad V\frac{dc_{\mathrm{B}}}{dt}=-AD_{\mathrm{B}c}\frac{\partial c'_{\mathrm{B}}}{\partial y} \tag{C3}$$

$$y = 0, \quad \frac{\partial c'_{\mathrm{B}}}{\partial y} = 0 \quad (\text{aqueous} - \text{catalyst interface}) \tag{C4}$$

These are converted into dimensionless parameters as follows

$$x \equiv \frac{y}{\delta_c}, \quad \tau \equiv \frac{D_{\mathrm{B}c}t}{\delta_c^2}, \quad u(x,\tau) \equiv \frac{c'_{\mathrm{B}}}{Kc_{\mathrm{B}o}}, \quad u_1 \equiv \frac{c_{\mathrm{B}}}{c_{\mathrm{B}o}},$$
$$\gamma \equiv \frac{KA\delta_c}{V}, \kappa \equiv \frac{k_{\mathrm{B}}\delta_c^2}{D_{\mathrm{B}C}} \tag{C5}$$

$$\frac{\partial^2 u}{\partial x^2} - \kappa u = \frac{\partial u}{\partial \tau}, \quad \tau > 0, \quad 0<x<1 \tag{C6}$$

$$x = 0, \quad \frac{\partial u}{\partial x} = 0; \tag{C7}$$

$$x = 1, \quad -\gamma\frac{\partial u}{\partial x} = \frac{du_1}{d\tau}, \quad u(1,\tau) = u_1(\tau) \tag{C8}$$

The operator $\mathbf{L} \equiv \{L,D(L)\}$ where $D(L)$ is the same as in the case to find the diffusion coefficient of benzaldehyde in catalyst phase but L is alerted to the following

$$L \equiv \begin{bmatrix} -\frac{d^2}{dx^2} - \kappa & 0 \\ \gamma\left(\frac{d}{dx}\right)_{x=1} & 0 \end{bmatrix} \tag{C9}$$

The eigenvalue problem is given by

$$\mathbf{Lz} = \lambda\mathbf{z} \Rightarrow z'' = -(\lambda+\kappa)z \tag{C10}$$

$$\gamma z'(1) = \lambda z_1 = \lambda z(1) \tag{C11}$$

$$z'(0) = 0, \quad z(1) = z_1 \tag{C12}$$

$$z(x) = A\cos\sqrt{\lambda+\kappa}x, \quad z_1 = A\cos\sqrt{\lambda+\kappa} \tag{C13}$$

$$\mathbf{z}_n \equiv A_n\begin{bmatrix} \cos\sqrt{\lambda_n+\kappa}x \\ \cos\sqrt{\lambda_n+\kappa} \end{bmatrix} \tag{C14}$$

$$-\gamma\sqrt{\lambda+\kappa}\sin\sqrt{\lambda+\kappa} = \lambda\cos\sqrt{\lambda+\kappa} \tag{C15}$$

$$\tan\sqrt{\lambda+\kappa} = -\frac{\lambda}{\gamma\sqrt{\lambda+\kappa}} \tag{C16}$$

$$\mathbf{u}(\tau) \equiv \begin{bmatrix} u(x,\tau) \\ u_1(\tau) \end{bmatrix} = \sum_{n=1}^{\infty}\langle u_0, z_n\rangle e^{-\lambda_n\tau}\begin{bmatrix} z_n(x) \\ z_{n1} \end{bmatrix} \tag{C17}$$

$$u(x,\tau) = \sum_{n=1}^{\infty}\frac{A_n\cos\sqrt{\lambda_n+\kappa}}{\gamma}e^{-\lambda_n\tau}A_n\cos\sqrt{\lambda_n+\kappa}x \tag{C18}$$

For large enough τ, we have the result

$$u(x,\tau) \approx \frac{(\lambda_n+\kappa)e^{-\lambda_n\tau}}{3\gamma^2(\lambda_n+\kappa)+\lambda_n(\lambda_n-\gamma)} \tag{C19}$$

Appendix D

Model for dispersed phase mixing and reaction

Consider a drop with volume v and outer catalyst layer thickness of δ_c. The concentration of B (benzaldehyde) in the drop changes by reaction at the catalyst phase by reaction to mandelic acid as well as to benzoic acid (very small amount). Denoting, the concentration of Benzaldehyde in organic phase by c_{B} and that in the catalyst phase by c'_{B}, the differential equations to be solved are as follows

$$\frac{\partial c_{\mathrm{B}}}{\partial t} = \frac{D_{\mathrm{B}}}{r^2}\frac{\partial}{\partial r}\left(r^2\frac{\partial c_{\mathrm{B}}}{\partial r}\right), \quad 0<r<R, \quad t>0 \quad R \equiv \left(\frac{3v}{4\pi}\right)^{1/3} \tag{D1}$$

$$\frac{\partial c'_{\mathrm{B}}}{\partial t} = \frac{D_{\mathrm{B}c}}{r^2}\frac{\partial}{\partial r}\left(r^2\frac{\partial c'_{\mathrm{B}}}{\partial r}\right) - k_{\mathrm{B}}c'_{\mathrm{B}}, \quad R<r<R+\delta_c, \quad t>0 \tag{D2}$$

$$t = 0, \quad c_{\mathrm{B}} = c_{\mathrm{B}_o}(0<r<R); \quad c'_{\mathrm{B}} = c_{\mathrm{B}_o}/K, \quad (R<r<R+\delta_c) \tag{D3}$$

The boundary and interface conditions are given by

$$r = 0, \quad \frac{\partial c_{\mathrm{B}}}{\partial r} = 0; \tag{D4}$$

$$r = R, \quad c_{\mathrm{B}} = Kc'_{\mathrm{B}}, \quad -D_{\mathrm{B}}\frac{\partial c_{\mathrm{B}}}{\partial r} = -D_{\mathrm{B}c}\frac{\partial c'_{\mathrm{B}}}{\partial r} \tag{D5}$$

$$r = R+\delta_c, \quad \frac{\partial c'_{\mathrm{B}}}{\partial r} = 0 \tag{D6}$$

assuming no surface reaction. Using the dimensionless variables

$$\tau \equiv \frac{D_{\mathrm{B}}t}{R^2}, \quad x \equiv \frac{r}{R}, \quad u_1 \equiv \frac{c_{\mathrm{B}}}{c_{\mathrm{B}_o}}, \quad u_2 \equiv \frac{c'_{\mathrm{B}}}{c_{\mathrm{B}_o}/K} \tag{D7}$$

we have the boundary-initial value problem

$$\frac{\partial u_1}{\partial \tau} = \frac{1}{x^2}\frac{\partial}{\partial x}\left(x^2\frac{\partial u_1}{\partial x}\right), \quad \tau > 0, \quad 0<x<1 \tag{D8}$$

$$\frac{\partial u_2}{\partial \tau} = \frac{\theta}{x^2}\frac{\partial}{\partial x}\left(x^2\frac{\partial u_2}{\partial x}\right) - \kappa u_2, \quad \tau > 0, \quad 1<x<1+\varepsilon \tag{D9}$$

$$\varepsilon \equiv \frac{\delta_c}{R}, \quad \kappa \equiv \frac{k_{\mathrm{B}}R^2}{D_{\mathrm{B}}}, \quad \theta \equiv \frac{D_{\mathrm{B}c}}{D_{\mathrm{B}}} \tag{D10}$$

$$u(x,0) = 1 \tag{D11}$$

$$x = 0, \quad \frac{\partial u_1}{\partial x} = 0; \tag{D12}$$

$$x = 1, \quad u_1 = u_2, \quad -\frac{\partial u_1}{\partial x} = -\frac{\theta}{K}\frac{\partial u_2}{\partial x} \tag{D13}$$

$$x = 1+\varepsilon, \quad \frac{\partial u_2}{\partial x} = 0 \tag{D14}$$

We define the operator $\mathbf{L} \equiv \{L,D(L)\}$ in the Hilbert space H such that

$$L \equiv -\frac{1}{r(x)}\frac{d}{dx}\left[p(x)\frac{d}{dx}\right] + q(x) \tag{D15}$$

such that

$$p(x) = \begin{cases} x^2, & 0<x<1 \\ \theta x^2, & 1<x<1+\varepsilon \end{cases} \tag{D16}$$

$$q(x) \equiv \begin{cases} 0, & 0<x<1 \\ \kappa, & 1<x<1+\varepsilon \end{cases} \tag{D17}$$

$$r(x) = \begin{cases} x^2, & 0<x<1 \\ \rho x^2, & 1<x<1+\varepsilon \end{cases} \tag{D18}$$

where

$$\rho = \frac{1}{K} \tag{D19}$$

$$u_1(x,\tau) = \sum_{n=1}^{\infty} \left\langle \mathbf{u}_o, \mathbf{z}_n \right\rangle z_{1,n}(x) e^{-\lambda_n \tau}, \quad 0<x<1 \tag{D20}$$

$$u_2(x,\tau) = \sum_{n=1}^{\infty} \left\langle \mathbf{u}_o, \mathbf{z}_n \right\rangle z_{2,n}(x) e^{-\lambda_n \tau}, \quad 0<x<1 \tag{D21}$$

where $\{\lambda_n, \mathbf{z}_n\}$ are infinite eigenvalues of $\mathbf{L}$, obtained by solving

$$\mathbf{Lz} = \lambda \mathbf{z}, \quad \mathbf{z} = \left\{ z(x) = \begin{cases} z_1(x), & 0<x<1 \\ z_2(x), & 1<x<1+\varepsilon \end{cases} \right\} \tag{D22}$$

which yields

$$\left(x^{-2} z_1'\right)' = -\lambda x^2 z_1, \qquad 0<x<1 \tag{D23}$$

$$\left(x^{-2} z_2'\right)' = -\left(\frac{\lambda}{\theta} - \kappa\right) x^2 z_2, \qquad 1<x<1+\varepsilon \tag{D24}$$

Eq. (D23) can be readily solved subject to the zero gradient boundary condition at $x = 0$ to get

$$z_1(x) = A x^{-1} \sin \sqrt{\lambda} x \tag{D25}$$

Eq. (D24) can be readily solved subject to the zero-gradient boundary condition at $x = 1 + \varepsilon$ to get

$$z_2(x) = B x^{-1} \left[\sin \sqrt{\frac{\lambda}{\theta} - \kappa}(1+\varepsilon-x) - (1+\varepsilon) \sqrt{\frac{\lambda}{\theta} - \kappa} \cos \sqrt{\frac{\lambda}{\theta} - \kappa}(1+\varepsilon-x) \right] \tag{D26}$$

The interface condition $z_1(1) = z_2(1)$ gives

$$A \sin \sqrt{\lambda} = B \left[\sin \varepsilon \sqrt{\frac{\lambda}{\theta} - \kappa} - (1+\varepsilon) \sqrt{\frac{\lambda}{\theta} - \kappa} \cos \varepsilon \sqrt{\frac{\lambda}{\theta} - \kappa} \right] \tag{D27}$$

The second interface condition is given by $K z_1'(1) = \theta z_2'(1)$ which gives

$$\begin{aligned} KA\left(-\sin\sqrt{\lambda} + \sqrt{\lambda}\cos\sqrt{\lambda}\right) &= \theta B \left\{ -\sin\varepsilon\sqrt{\frac{\lambda}{\theta}-\kappa} - \sqrt{\frac{\lambda}{\theta}-\kappa}\cos\varepsilon\sqrt{\frac{\lambda}{\theta}-\kappa} + \right. \\ &+ (1+\varepsilon)\sqrt{\frac{\lambda}{\theta}-\kappa}\cos\varepsilon\sqrt{\frac{\lambda}{\theta}-\kappa} - (1+\varepsilon)\left(\frac{\lambda}{\theta}-\kappa\right) \\ &\left. \sin\varepsilon\sqrt{\frac{\lambda}{\theta}-\kappa} \right\} \end{aligned} \tag{D28}$$

The characteristic equation for the eigenvalues is

$$\sqrt{\lambda}\cot\sqrt{\lambda} - 1 = \frac{\frac{\theta}{K}\left[\varepsilon\sqrt{\frac{\lambda}{\theta}-\kappa}\cot\left(\varepsilon\sqrt{\frac{\lambda}{\theta}-\kappa}\right) - \left\{1+(1+\varepsilon)\sqrt{\frac{\lambda}{\theta}-\kappa}\right\}\right]}{\left[1-(1+\varepsilon)\sqrt{\frac{\lambda}{\theta}-\kappa}\cot\left(\varepsilon\sqrt{\frac{\lambda}{\theta}-\kappa}\right)\right]} \tag{D29}$$

The final solution of the boundary initial value problem is given by

$$\bar{u}(\tau) = \sum_{n=1}^{\infty} e^{-\lambda_n \tau} \frac{\langle \mathbf{1}, \mathbf{z}_n \rangle^2}{\langle \mathbf{1}, \mathbf{1} \rangle} \tag{D30}$$

The following model is considered when the diffusion effects become negligible. The coalescence and redispersion process results in mixing of the contents of the droplets. From the experimental data on diffusivity of benzaldehyde in organic phase and the reaction time, it was observed that the time scale of diffusion is very less than the time scale of reaction, so it can be assumed that benzaldehyde is spread uniformly in the organic phase and the catalyst-rich phase and attains equilibrium quickly.

At any instant, the concentration is assumed uniform in the organic phase as well as the catalyst-rich phase surrounding the droplet. For a droplet of volume $v = \frac{4\pi}{3}R^3$ with catalyst thickness δ_c, and volume v_c

$$v_c \equiv \frac{4\pi}{3}\left[(R+\delta_c)^3 - R^3\right] = \frac{4\pi R^3}{3}\left[(1+\varepsilon)^3 - 1\right] = 3v\varepsilon\left(1+\varepsilon+\frac{\varepsilon^2}{3}\right) \tag{D31}$$

If the concentration of benzaldehyde in the hexane core of the drop is assumed to be uniform at c_B, then the concentration in the catalyst layer at equilibrium is uniformly c_B/K. The mass balance may then written for the droplet as

$$\frac{d}{dt}\left[v c_B + v_c c_B/K\right] = -v_c k c_B/K \tag{D32}$$

In terms of the dimensionless variables used in the diffusion-reaction formulation, we may rewrite D32 as

$$\frac{d\bar{u}}{d\tau} = -\frac{\kappa}{1+K(v/v_c)}\bar{u} \tag{D33}$$

$$\bar{u}(0) = 1 \tag{D34}$$

The solution is written in lieu of (D31) as

$$\bar{u}(\tau) = \exp\left[-\tau\frac{\kappa\{3\varepsilon(1+\varepsilon+\varepsilon^2/3)\}}{K+\{3\varepsilon(1+\varepsilon+\varepsilon^2/3)\}}\right] \tag{D35}$$

Manuscript received Oct. 16, 2011, revision received Nov. 3, 2011, and final revision received Feb. 7, 2012.